Single-Cell RNA-Seq Analysis of Diabetic Wound Macrophages in STZ-Induced Mice

Siyuan Yin
Shandong University Cheeloo College of Medicine
Jiaxu Ma
Shandong University Cheeloo College of Medicine
Ru Song
Shandong University Cheeloo College of Medicine
Chunyan Liu
Shandong Qianfoshan Hospital
Guoqi Cao
Shandong University Cheeloo College of Medicine
Guang Zhang
Shandong University Cheeloo College of Medicine
Zhenjie Wu
Shandong University Cheeloo College of Medicine
Huayu Zhang
Shandong University Cheeloo College of Medicine
Rui Sun
Shandong University Cheeloo College of Medicine
Aoyu Chen
Shandong First Medical University
Yibing Wang (ybwang@sdfmu.edu.cn)
The first Affiliated Hospital of Shandong First Medical University & Shandong. Provincial Qianfoshan Hospital https://orcid.org/0000-0002-0012-4455

Research

Keywords: Macrophage, single-cell RNA sequencing, chronic wound.

Posted Date: November 30th, 2021

DOI: https://doi.org/10.21203/rs.3.rs-1100779/v1

Abstract

Background: The crucial role of macrophages in the healing of chronic diabetic wounds is widely known, but previous in vitro classification and marker genes of macrophages may not be fully applicable to cells in the microenvironment of chronic wounds. The heterogeneity of macrophages was studied and classified at the single-cell level in a chronic wound model.

Results: We performed single-cell sequencing of CD45+ immune cells within the wound edge and obtained 17 clusters of cells, including 4 clusters of macrophages. One of these clusters is a previously undescribed population of macrophages possessing osteoclast gene expression, for which analysis of differential genes revealed possible functions. We also analysed the differences in gene expression between groups of macrophages in the control and diabetic wound groups at different sampling times.

Conclusions: we described the differentiation profile of mononuclear macrophages, which has provided an important reference for the study of immune-related mechanisms in diabetic chronic wounds.

Background

The clinical treatments for chronic wound remain ineffective, and the dramatic increase in healthcare costs has created a heavy financial strain, with total US Medicare treatment costs for trauma-related care ranging from $28.1 to $96.8 billion in 2018 statistics, in which diabetic ulcers and surgical trauma were the most costly[1]. From the 2017–2020 US reported statistics, the 5-year survival rate for diabetic foot was 30.5%, which was similar to the 5-year survival rate for cancer combined of 31%, while in terms of care, diabetes care was more expensive, and a significant amount of funding was consumed for lower extremity care[2]. The ageing population has a high prevalence of chronic wound, and ageing is becoming an important worldwide healthcare and demographic issue[3]. Projections indicate that in 2050, there will be more older people aged 60 years or older than adolescents aged 10–24 years (2.1 billion versus 2 billion)[4]. The global market for advanced wound care is expected to reach US$18.7 billion by 2027, growing at a compound annual growth rate (CAGR) of 6.6% during the analysis period 2020–2027[5]. Diabetic patients and obese individuals are at high risk of chronic wounds. Chronic inflammation is also an important cause of chronic wound in diabetes due to the long-term effects of high sugar and free fatty acids, which lead to a chronic inflammatory state in a variety of tissues. Chronic inflammation in diabetes can be manifested by the recruitment of immune cells such as macrophages and neutrophils to tissues and the release of proinflammatory cytokines[6]. The current classification of macrophages as an important part of immune cells has revealed some differences in vitro and in vivo, and the previous markers for typing these cells are not well suited for the current study[7]. Single-cell sequencing, a new technology that has emerged in recent years[8], provides a way to classify and functionally study cell populations in specific microenvironments independent of prior experience[9, 10]. Using the 10X genomics single-cell platform[11, 12], we performed unbiased analysis of CD45+ immune cells from the skin of STZ-induced C57BL/6J mice and wild-type mice in a whole skin wound model to

discover the distribution of the different populations of immune cells, as well as the genetic profile of trauma-associated macrophages and analysed their temporal genetic differences.

Materials And Methods

Animals

In this study, male C57BL/6J mice (n = 60) weighing 20–25 g were used. All experimental protocols were approved by the ethics committee of Shandong Qianfoshan Hospital, Shandong University, and all experiments were performed according to the approved protocols. Mice were housed under controlled temperature (26 ± 1.5°C) and humidity (60% ± 5) with a 12-h light/dark schedule.

Development of the diabetic mouse model

Streptozotocin (120 mg/kg, Sigma-Aldrich, USA, S0130) was administered to 4-week-old C57BL6J mice after 12 h of fasting. Blood glucose was measured after 7 days of stabilization, and mice with glucose levels ≥16.5 mmol/L (300 mg/dL) were considered diabetic and were used for the operation.

Wound sampling

Diabetic mice (n=20) and control mice (n=20) were anaesthetized with isoflurane inhalation, and then the hair on the back was removed to create a full skin wound 5 mm in diameter, which was observed daily. The mice were sacrificed on day 1, day 3, day 5 and day 7, and wound tissue was obtained.

Preparation of single-cell suspensions

The digestion solution was composed of collagenase II (3.5 mg/mL, Solarbio, China), DNase I (0.02 mg/mL, Solarbio, China), hyaluronidase (30 U/mL, Solarbio, China), 5% FBS-1640 (Gibco, USA), and DPBS (Gibco, USA). Samples were washed, the digestion solution was added to the tissue, and the tissue was cut and incubated at 37°C for 1 h. The digestion solution was passed through a 40-μm cell strainer and then centrifuged at 500 x g for 5 min. The reaction was terminated by adding erythrocyte lysate for 5 min and centrifuging twice at 300 x g for 5 min.

Flow sorting

A portion of the cell suspension was centrifuged at 300 x g for 5 min. One hundred microlitres of wash solution was used to resuspend the cell precipitate, 2 μL of APC anti-mouse CD45 antibody (BioLegend, USA) was added for every 1E6 cells according to the total number of cells, and the mixture was incubated at 4°C and protected from light for a total incubation time of 30 min. At 15 min of incubation time, 1 μL of calcein AM (BD, USA) was added for every 100 μL of cell suspension. After incubation, the cells were washed twice by centrifugation at 300 x g for 5 min; the supernatant was discarded, and the cells were resuspended and mixed with the appropriate amount of washing solution. A small amount of the suspension was stained with AO/PI, and the number of cells sorted, the cell viability and the clumping

rate were recorded; the cells were centrifuged at 300 x g for 5 min and resuspended in sample buffer for BD quality control.

Single-cell RNA-sequencing (scRNA-seq)

The scRNA-seq libraries were prepared according to the protocol of the Chromium Single-cell 3' Reagent V3 Kit manufacturer (10× Genomics). Single-cell suspensions were then added to the Chromium Single-Cell Controller Instrument (10× Genomics) to generate single-cell gel bead emulsions (GEMs). Finally, these libraries were sequenced on an Illumina sequencing platform (HiSeq X Ten), and 150-bp paired-end reads were obtained. In the above process, each mRNA is randomly ligated with a unique molecular identifier (UMI) after reverse transcription, by which the number of mRNAs can be counted.

Data analysis

The main tools and R packages used or bioinformatic analysis are Cell Ranger (Version 3.0.0), Seurat (Version 4.0.3), Monocle (Version 2.20.0), clusterProfiler (Version 4.0.2), and ggplot2 (Version 3.3.5).

Results

We performed scRNA-seq on CD45+ cells gathered from wound tissue obtained from wild-type and STZ-induced diabetic C57BL/6J mice (Fig. 1a). Four time points were selected for sampling (1, 3, 5, and 7 days). The single-cell data of the obtained samples were normalized by excluding low-quality cells to eliminate batch effects, and data from a total of 9240 cells were obtained. Principal component analysis (PCA) was performed, and the results were plotted with t-stochastic neighbour embedding (t-SNE) downscaled to show the distribution of cells from different sample sources in the overall data (Fig. 1b), along with the gene expression level of all single cells and the number of their UMI expressed (Fig. 1c).

QC cell data were unbiased using the Seraut package, and gene expression data from cells extracted from both conditions were aligned and projected in a 2D space through t-SNE to allow identification of overlapping and diabetic wound-associated immune cell populations. A total of 17 cell clusters were obtained, except for low-quality cells, which have a high preponderance of mitochondrial genes (Fig. 2a). We mapped the heat map of major marker genes in all populations. (Fig. 2b) The cell populations obtained were 4 clusters of neutrophils (cluster 0, cluster 1, cluster 3 and cluster 12, with marker genes Ptprc, S100a8, s100a9, Csf3r, Cxcr2, and Lrg1); 2 clusters of monocytes (cluster 6 and cluster 8, with marker genes Ly6c2, Vcan, and Fn1); 3 clusters of macrophages (cluster 2, cluster 4, and cluster 9, with marker genes C1qa and Mrc1); 2 clusters of DC cells (cluster 5 and cluster 13, with marker genes Ccr7, Mgl2, Ccl22 Cd209a, and Fscn1), 1 cluster of NK cells (cluster 14, with marker genes Cd3d-, Xcl1, and Ncr1); 1 cluster of T cells (cluster 7, with the main marker genes Cd3d, Cd3e, Cd3g, and Trac); 1 cluster of mast cells (cluster 16, with the main marker genes Ms4a2, Cpa3, Gata2, and Tpsb2); 1 cluster of fibroblasts (cluster 17, with the main marker genes Col1a1 and Dcn); and 1 cluster of cells not previously described (cluster 11), with the main marker genes Acp5, Ctsk, Mmp9, Top2a, and Mki67, which are noted in the literature as marker genes for osteoclasts (Fig. 2c).

To characterize cluster 11 as a specific group of immune cells, we mapped the top 20 marker genes on a violin plot (Fig. 3a) and performed GO functional enrichment analysis of the marker genes. The genes that were highly expressed were the osteoclast-associated genes Ctsk and Acp5; the adipose tissue-associated genes Hmgn1, Ranbp1 and Lpl; and the macrophage-associated genes Tsc22d1 and Banf1. The cycling basal cell-related genes Stmn1, Top2a, Ube2c, Pclaf, and Birc5 suggest that this group of cells may be a previously undescribed type of skin-resident macrophage. The GO functional enrichment analysis results showed that the gene functions were mainly related to translation, RNA splicing, mRNA processing, rRNA processing, oxidation-reduction process, translational initiation tricarboxylic acid cycle, cell cycle, protein folding, transport, etc. (Fig. 3b)

We further compared the gene expression differences between cluster 11 and all other macrophages (cluster 2, cluster 4, and cluster 9). A total of 230 genes were upregulated and 205 genes were downregulated in cluster 11 compared to the other macrophage populations (Fig. 3c). GO enrichment of the differential genes showed that upregulated genes were enriched in tissue remodeling, skeletal system development, multicellular organismal homeostasis, cation transmembrane transport, cation transport, collagen metabolic process, bone resorption, bone remodeling, porton transmembrane transport, and tissue homeostasis (Fig. 3d). Biological functions of the downregulated genes are enriched in defense response, immune response, inflammatory response, response to bacterium, leukocyte migration, myeloid leukocyte migration, cell chemotaxis, granulocyte migration, neutrophil migration, and granulocyte chemotaxis (Fig. 3e).

We observed that the differentially expressed genes in cluster 11 were enriched in multiple metabolic pathways, and we generated a metabolism heatmap for all cell populations. The gene metabolism patterns of cluster 11 were high enriched in one-carbon pool by folate, vitamin B6 metabolism, lipoic acid metabolism, synthesis and degradation of ketone bodies, citrate cycle, oxidative phosphorylation, 2-oxocarboxylic acid metabolism, carbon metabolism, pyruvate metabolism, fatty acid biosynthesis, and cysteine and methionine metabolism. Among the remaining macrophage populations, cluster 4 and cluster 9 showed some similarity in gene metabolism patterns and differed significantly from cluster 2. The similarities between cluster 4 and cluster 9 were mainly enriched in caffeine metabolism, glycosphingolipid biosynthesis – globo and isoglobo series, sphingolipid metabolism, other glycan degradation, glycosaminoglycan degradation, ascorbate and aldarate metabolism, and glycosphingolipid biosynthesis – ganglio series (Fig. 4a).

The violin plots for the marker genes expressed in cluster 2, cluster 4, and cluster 9 showed that cluster 4 expressed genes that were similar to those previously defined as “M2 macrophages” (Mrc1 and cd163). Cluster 2 had more proinflammatory genes, and the genes cd74, tnsf9, tnsf12, and tnsf12a were highly expressed.Gene expression of Gpnmb,Pf4,Lpl,Cd36,Apoe were found more significant in cluster9.Fig. 4b,4c,4d

The phenotypic changes and overall proportional changes in macrophages in the two different subgroups are also an important part of our understanding of their mechanisms. Thus, we counted the

proportional changes in the macrophage populations in the two experimental groups at different sampling times, and the proportion of the cluster 11 cell population increased in the early stage (day 1–day 3) in both the diabetic wound group and the control group, but unlike the diabetic wound group, the proportion of this cell population in the control group increased consistently (1.26%) on day 5 and was much higher than that in the diabetic wound group (0.08%) and decreased (0.28%) on day 7, but the proportion was still higher than that of the diabetic group (0.08%) (Fig. 5A). The proportion of Cluster 2 cells was higher in diabetic groups on day 1(0.85% verses 0.41%), with similar trends in cell proportions within both groups. After day 3 the proportion of cluster2 cells was higher in the control wound group than in the diabetic wound group (1.42% verses 0.73%). Cluster 4 showed a gradual increase in the proportion of cells in the diabetic wound group, except on day 5. In the control group, however, a much higher increase was observed on day 5 (3.14%) and day 7 (8.09%) than that in the diabetic group. A peak in the proportion of cluster 9 was observed in the diabetic group (1.07%) at an earlier time point (on day 3) than in the control group (1.22% on day 5) (Fig. 5B).

It is well known that the immune environment of the diabetic group differs from that of the normal group, so the specific differences in the macrophage population at different time points are of interest to us. In the next step, we performed GO enrichment analysis of the differential genes and found that the differences in the biological functions between the two groups with respect to cluster 11 on day 3 were mainly enriched in immune system process, response to external stimulus, regulation of immune system process, regulation of neuron death, defence response to bacterium, and cellular response to oxidative stress (Fig. 5C). The biological functions of the downregulated genes in cluster 11 on day 5 in the diabetes group were enriched in positive regulation of protein modification process, positive regulation of cell communication, positive regulation of protein phosphorylation, positive regulation of phosphorus metabolic process, negative regulation of cell death, and blood vessel morphogenesis (Fig. 5D).

KEGG analysis of the day 3 differentially expressed genes corresponded to rheumatoid arthritis, lipid and atherosclerosis, and the Toll-like receptor signalling pathway (Fig. 5E). The day 7 upregulated genes in the diabetes group corresponded to type I diabetes and Th17 cell differentiation (Fig. 5F).

GO analysis of the differential genes in cluster 2 at day 3 in two wound groups showed enrichment of biological functions in response to stress, defence response, response to external stimulus, response to external biotic stimulus, response to other organism, response to biotic stimulus, interspecies interaction between organisms, response to bacterium, immune response, inflammatory response, and defence response to other organism. Downregulated gene functions in the diabetic group were enriched in cytokine production and regulation of cytokine production (Supplementary 1).

KEGG analysis showed differential gene enrichment in the cholesterol metabolism pathway, which was downregulated by day 5 in the diabetes group (Supplementary 1).

The biological functions of the cluster 4 differentially expressed genes on day 1 were enriched in positive regulation of developmental process, regulation of apoptotic signalling pathway, negative regulation of apoptotic signalling pathway, interleukin-1 beta production, and interleukin-1 production. The day 3

differential genes were enriched in response to external stimulus, defence response, interspecies interaction between organisms, response to external biotic stimulus, response to other organism, and inflammatory response (Supplementary 2). The biological functions of the upregulated genes at day 5 in the diabetic group were enriched in response to external biotic stimulus, response to other organism, response to biotic stimulus, interspecies interaction between organisms, innate immune response, defence response to other organism, and response to lipopolysaccharide (Fig. 5G).

The KEGG enriched differential gene pathways on day 5 were autoimmune thyroid disease, allograft rejection, graft-versus-host disease, type 1 diabetes mellitus, antigen processing and presentation, systemic lupus erythematosus, Staphylococcus aureus infection, and viral myocarditis (Fig. 5H).

The downregulated genes in cluster 9 in the diabetes group on day 1 were enriched in response to external biotic stimulus, response to other organism, response to biotic stimulus, defence response (Supplementary 3). The downregulated genes at day 3 were functionally enriched in tissue development, leukocyte differentiation, blood vessel development, vasculature development, cellular response to growth factor stimulus, and response to growth factor positive regulation of endothelial cell proliferation. The upregulated gene functions on day 5 were enriched in positive regulation of response to external stimulus, regulation of hydrolase activity, granulocyte chemotaxis, granulocyte migration, regulation of peptidase activity, myeloid leukocyte migration, and leukocyte chemotaxis (Supplementary 3). The downregulated genes at day 7 were enriched in biological functions including response to abiotic stimulus, cellular response to stress, positive regulation of pri-miRNA transcription by RNA polymerase II, and positive regulation of neuron death (Supplementary 3).

The KEGG analysis showed that the downregulated genes at day 3 were involved in the MAPK signalling pathway, relaxin signalling pathway, chemical carcinogenesis-receptor activation, and rheumatoid arthritis. The downregulated genes at day 7 were enriched in the oestrogen signalling pathway, measles, MAPK signalling pathway, lipid and atherosclerosis, prion disease, human T-cell leukaemia virus 1 infection, endocrine resistance, and antigen processing and presentation (Supplementary 3).

Monocytes can differentiate into macrophages during the immune process, and macrophages have rich phenotypic diversity and perform different functions at different times during wound healing. We performed a chronological analysis of the observed mononuclear macrophage population and the cells in the diabetic and normal trauma groups could be classified into 11 states (Fig. 6A, 6B). According to the pseudotime analysis (Fig. 6C, 6D), cluster 6 and cluster 8 were predominantly found in the early states, followed by cluster 2, and cluster 4 and cluster 9 were found in large numbers at later time points. In the diabetic wound group, a large number of cluster 4 cells were observed in only one state, whereas in the control group, cluster 4 cell aggregates were observed in several states. In contrast, in the diabetic group, cluster 2 was observed within multiple stages of differentiation (Fig. 6E, 6F). This finding suggests that within the diabetic group, cell differentiation was more towards cluster 2, whereas in the control group, more branches were differentiated into cluster 4, and the greatest number of cluster 4 aggregates could

be seen in the diabetic group with a branch point of 3 compared to 1 in the control group, leading us to more closely analyse the differential gene expression patterns of the two trajectory branches.

In branch 1 of the control group and branch 3 of the diabetic group, a pattern of differential expression consisting of the grouping of genes with a reduction in the differentiation pathway towards cluster 4 and an elevation of the differentiation pathway towards cluster 2 can be observed, with such a pattern seen in branch3 of the diabetic group for Acod1, Slc7a11, il1a, spp1, Ccdc71l, Tnbs1, F10, Ptgs2, Chil3, Met, and Cxcl3 (Fig.6G). In the control group, there were Tgfbi, cd52, plac8, lfi2712a, plbd1, lmnb1, gpr132, lsp1, ly6a, ccr2, and cytip in branch1 (Fig.6H). No crossover genes were found, suggesting that the polarization patterns of macrophages in the control and diabetic group may be quite different.

Discussion

Using single-cell sequencing unbiased analysis, we described immune cell populations within the wound-associated cells of STZ-induced diabetic and normal mice and defined a population of macrophages expressing osteoclast cell marker genes. The proportion of cd45+ immune cells within the skin was also found to vary between populations at different time points. We proximally analysed the differences in gene expression in macrophage populations at different sampling points and found evidence of temporal variation in the effects of immune dysfunction on wound healing in diabetic mice. The differences in the developmental differentiation trajectory of mononuclear macrophages were also analysed to describe specific differential genes at the macrophage differentiation and polarization branching points.

Our wound-associated macrophage profile yielded three classes of macrophages, with cluster 2 macrophages expressing the cd74, tnfsf9, tnfsf12, and tnfrsf12a genes, suggesting their potential for proinflammatory function. Cd74 is a high affinity receptor on the cell membrane that binds macrophage migration inhibitory factor (MIF)[13] The interaction of MIF with CD74 can occur at an early stage as a manifestation of the cellular response to injury. CD74 is involved in numerous inflammatory-related disease processes, and recent studies in inflammatory bowel disease (IBD) have shown a strong association between CD74 polymorphisms and the failure of anti-TNF therapy in patients with ulcerative colitis[14]. In a mouse model of experimental ischaemia-reperfusion injury, renal tubular injury was more severe in MIF, MIF-2 and CD74 knockout mice than in wild-type control mice[15], and the autoimmune disease systemic lupus erythematosus (SLE) can cause renal inflammation known as lupus nephritis[16]. In mouse models of SLE, researchers have observed elevated levels of CD74 expression in B lymphocytes, and elevated MIF has been demonstrated in lupus-prone strains of mice. Inhibition of MIF and knockdown of CD74 protect against glomerulonephritis in lupus-susceptible mice[17, 18]. CD74 has been less well reported in skin tissue injury, but there is previous evidence in early animal skin injury models that MIF-CD74 promotes the proliferation and migration of keratinocytes at the trabecular margin[19]. In our experiments, KEGG pathway enrichment analysis suggested that the difference in the LPL gene expression between the wound groups at day 5 was related to the cholesterol metabolic pathway, perhaps leading to a greater response to inflammation in the diabetic wound group than in the control group. Tests of macrophage depletion in wounds at different time points have also shown that

early depletion of macrophage populations significantly contributed to delayed wound healing but could attenuate late scar formation[20]. This finding suggests that CD74+ immune cells may have different roles within different tissues and in different immune settings. In our present results, CD74high macrophages were observed in the early stages in both groups of samples, with the normal group having a lower responsiveness than the diabetic group on the first day and a higher overall proportion in the normal group at the later stages. This group of macrophages was also observed to express Tgfbi. As CD74high macrophages appear at an early stage as a high proportion of the macrophages, it remains to be investigated whether modulation of CD74 expression can influence scar formation.

Cluster 4 cells expressed the mrc1-cd206, il-10, cd163 and cbr2 genes, with gene expression patterns similar to those traditionally described for M2 macrophages, while cluster 4 cells also expressed the F13a1, lyve1, and gas6 resident-like macrophage genes[21, 22]. Notably, when comparing the differences in gene expression between cluster 4 cells from the diabetic and normal wounds, the diabetic group was found to express higher levels of Lyve1, while the normal group expressed higher levels of ccr2, suggesting that this group of cells with the M2 cell gene signature may have origins in both monocyte recruitment and resident macrophages[23]. In our experiments, the distribution of M2-like macrophages in both groups was much higher in the control group than in the diabetic group, suggesting that the normal group included resident macrophages and more differentiated monocytes recruited from the blood, whereas the M2-like macrophages in the diabetic group were more dependent on their own resident macrophages. A comparative analysis of the gene differences between the two groups at different time points showed that the expression of il-1 was promoted at an early stage in the diabetic group, and later, the diabetic group had a higher level of inflammatory response and defence function than the normal group. In contrast, in the normal group, the differential gene expression in the early phase was mainly enriched in the functions of proliferation and apoptosis regulation. Higher cd163 expression was observed in the diabetic group than in the normal group at both day 3 and day 7. It has also been suggested that sCD163 is higher in type 2 diabetes patients than in healthy individuals[24]. These results may suggest that the elevated feedback appearance of cd163 as an anti-inflammatory gene in macrophages is one of the protective mechanisms promoting wound repair in the diabetic group. The KEGG pathway analysis of the day 5 differential genes showed enrichment in type 1 diabetes and several pathways associated with autoimmune diseases in both groups, suggesting that immune disorders in diabetic patients are more prevalent in this group of macrophages.

Cluster 9 cells are highly similar to cluster 4 in their M2-like macrophage gene expression profile, with the difference being that cluster 9 is highly Gpnmb-expressing, and in tumour-related studies, the tumour-promoting role of myeloid cells is associated with Gpnmb, which can promote cancer cell survival, cancer stem cell expansion and metastatic phenotype acquisition via IL-33[25]. This ability to promote stemness was transduced in skin injury to promote stem cell proliferation and repair capacity in the skin, and transplantation of GPNMB-expressing macrophages improved skin healing in GPNMB-mutant mice. Furthermore, topical treatment with recombinant GPNMB restored mesenchymal stem cell recruitment, prompted polarization of wound macrophages towards anti-inflammatory M2 macrophages, and accelerated wound closure in diabetic skin[26]. It remains to be determined whether this group of cells

appearing in a higher abundance at the peak of the proportion of diabetic wounds (day 3) but at a lower level than that in the control group afterwards is the result of some inflammatory influence that hinders the proliferation and expression of this group of cells in the mid-term. Our results show that among the enriched GO biological functions of the differentially expressed genes in cluster 9 on day 3, the functions of the downregulated genes are associated with tissue repair, angiogenesis and development and cellular response to growth factors. It has been demonstrated that Junb knockout mice can develop normally, but a lack of Junb under wound conditions results in excessive epidermal skin proliferation and a delayed inflammatory disorder remodelling phase[27]. Nr4a1, a monocyte transition gene, has been shown to have an important role in genetic models and in the differentiation of monocytes/macrophages in the mouse intestine[28]. KEGG enrichment analysis suggests that the MAPK pathway may play a regulatory role in the proliferation and differentiation of this group of cells. According to the differential analysis, the elevated Gpnmb-high macrophage Tgfbi, IL10, and CD163 expression in the diabetic wound group on day 5 and day 7 may be a result of a delayed repair phase compared to the control group.

Osteoclast macrophages (cluster 11) are an interesting group of cells with high expression of the osteoclast-associated genes Ctsk and Acp5; the adipose tissue-associated genes Hmgn1, Ranbp1, and Lpl; the macrophage-associated genes Tsc22d1 and Banf1; and the cycling basal cell-associated genes Stmn1, Top2a, Ube2c, Pclaf, and Birc5. Under physiological conditions, macrophages and osteoclasts are part of the outcome of monocyte differentiation, and the main determinants of osteoclast production are the relative concentrations of CSF-1, RANKL and osteoprotegerin (OPG; TNF receptor superfamily member 11B)[29, 30]. In vitro stimulation of RAW264.7 macrophages with RANKL can result in osteoclasts[31][32]. Advanced glycation end products (AGEs) in the diabetic state can affect the expression of bone metabolism proteins[33]. Increased reactive oxygen species in diabetes can also affect the balance between osteoclasts and osteoblasts, leading to osteoporosis[34]. Chronic inflammatory skin diseases such as atopic dermatitis (AD) and psoriasis vulgaris (Pso) are associated with osteoporosis[35, 36]. Secondary osteoporosis occurs in a transgenic model of spontaneous dermatitis[37]. All of this evidence suggests that an increase in osteoclasts occurs in response to a strong inflammatory response and stimulation by proinflammatory factors. However, in our study, the proportion of macrophages with osteoclast markers was lower in diabetic mouse wounds with enhanced inflammatory responses, suggesting that, unlike the mechanism of cutaneous inflammation leading to arthritis and osteoporosis, this may be a localized form of cell differentiation specific to the skin.

Human bone, epidermis and hair are all lifelong renewable tissues, and perhaps due to this similarity, except for the role of NF-κB receptor activator (RANK) in osteogenesis and resorption, mice lacking RANK ligand (RANKL) are unable to initiate a new growth phase of the hair cycle and display stalled epidermal homeostasis. RANKL can be expressed in the skin by activated interfollicular epidermis[38], and RANK-RANKL regulates hair renewal and epidermal homeostasis and provides a communication channel between these two activities[39]. This regulatory ligand for long-term self-renewal may be responsible for the generation of our group of osteoclast-like macrophages. The metabolic pathways and differential gene enrichment results of this group of cells also suggest that they have a strong biosynthetic and metabolic capacity and that the response of this group is stronger in normal wounds, suggesting that

perhaps this class of skin-specific macrophages contributes to normal skin homeostasis and repair after damage.

There are still some limitations to this study. The time points chosen for this study are based on previous studies and animal studies and are still somewhat intermittent, as there may be specific peaks in immune cell changes and microenvironmental regulation that do not necessarily occur at the times we chose. The study was conducted at the transcriptional level only and did not include other factors that may affect macrophage function.

These macrophages vary in type and temporal characteristics, and the classical definitions describing the markers and classifications of classically activated macrophages and alternative activated macrophages, or M1 and M2 cells, do not seem to match the descriptions exactly. These results suggest that in vitro studies of immune cells with a single factor and a small number of markers may not accurately model the in vivo environment, especially when analysing the differences in their temporal patterns. More precise gene profiling of cells in vivo and improvements in the way in which they are tracked in vivo may better enable us to identify new immune regulatory mechanisms and therapeutic targets.

Conclusion

In summary, we characterized the genetic profile of macrophage populations in wounds of diabetic and normal mice by single-cell sequencing and identified a population of macrophages with osteoclast-like gene expression, presumably associated with skin renewal and repair responses. We described the genetic differences between the different cell populations in the wounds of the two groups according to chronological order, providing a closer look into specific processes. Some targets are important as reference makers for macrophages in the field of wound repair.

Abbreviations

STZ: Streptozocin

FBS: Fetal bovine serum

DPBS: Dulbecco's Phosphate Buffered Saline

GO: Gene Ontology

KEGG: Kyoto Encyclopedia of Genes and Genomes

Declarations

Ethics approval and consent to participate:

All experimental protocols were approved by the ethics committee of Shandong Qianfoshan Hospital, Shandong University, and all experiments were performed according to the approved protocols.

Consent for publication:

Not applicable.

Availability of data and materials:

All sequencing data were submitted to the BioProject of National Center for Biotechnology Information (NCBI), GEO Submission (GSE186821).

Competing interests:

The authors declare that they have no competing interests.

Funding:

This study was supported by the National Natural Science Foundation of China (81772092 and 81972947), Natural Science Foundation of Shandong Province of China (Major Basic Research Program) (ZR2019ZD38), “Academic Elevation Program” of Shandong First Medical University (Shandong Academy of Medical Sciences) (2019LJ005) and Jinan Clinical Research Center for Tissue Engineering Skin Regeneration and Wound Repair.

Author Contributions

Conceptualization: SY, YC, YW; Data Curation: SY, RS, JM, CL; Formal Analysis: SY, RS, JM; Funding Acquisition: YW; Investigation: SY, RS, JM, GC, GZ, ZW; Methodology: SY, RS, JM; Project Administration: SY, CL, YW; Resources: YC, CL, YW; Supervision: YW; Validation: HZ, RS, AC; Visualization: JM; Writing–original draft: JM; Writing–review & editing: CL, YW

Acknowledgements:

Not applicable.

Author information:

Department of Plastic Surgery, Shandong Provincial Qianfoshan Hospital, Cheeloo College of Medicine, Shandong University, Jinan, Shandong, 250012, P. R. China.

Ru Song Siyuan Yin, Jiaxu Ma, Guoqi Cao, Guang Zhang, Zhenjie Wu, Huayu Zhang, Rui Sun, Yibing Wang

Jinan Clinical Research Center for Tissue Engineering Skin Regeneration and Wound Repair, The First Affiliated Hospital of Shandong First Medical University & Shandong Provincial Qianfoshan Hospital,

Jinan 250014, P. R. China.

Ru Song Siyuan Yin, Jiaxu Ma, Chunyan Liu, Guoqi Cao, Guang Zhang, Zhenjie Wu, Huayu Zhang, Rui Sun, Aoyu Chen, Yibing Wang

Department of Plastic Surgery, The First Affiliated Hospital of Shandong First Medical University & Shandong Provincial Qianfoshan Hospital, Jinan 250014, P. R. China.

Siyuan Yin, Chunyan Liu, Aoyu Chen, Yibing Wang

References

1. S.R. Nussbaum, M.J. Carter, C.E. Fife, J. DaVanzo, R. Haught, M. Nusgart, D. Cartwright, An Economic Evaluation of the Impact, Cost, and Medicare Policy Implications of Chronic Nonhealing Wounds, Value Health 21(1) (2018) 27–32.
2. D.G. Armstrong, M.A. Swerdlow, A.A. Armstrong, M.S. Conte, W.V. Padula, S.A. Bus, Five year mortality and direct costs of care for people with diabetic foot complications are comparable to cancer, J Foot Ankle Res 13(1) (2020) 16.
3. OECD, Elderly population, 2014.
4. E. Rudnicka, P. Napierala, A. Podfigurna, B. Meczekalski, R. Smolarczyk, M. Grymowicz, The World Health Organization (WHO) approach to healthy ageing, Maturitas 139 (2020) 6–11.
5. C.K. Sen, Human Wound and Its Burden: Updated 2020 Compendium of Estimates, Adv Wound Care (New Rochelle) 10(5) (2021) 281–292.
6. R. Pahwa, A. Goyal, P. Bansal, I. Jialal, Chronic Inflammation, StatPearls, Treasure Island (FL), 2021.
7. M. Orecchioni, Y. Ghosheh, A.B. Pramod, K. Ley, Macrophage Polarization: Different Gene Signatures in M1(LPS+) vs. Classically and M2(LPS-) vs. Alternatively Activated Macrophages, Front Immunol 10 (2019) 1084.
8. A.E. Saliba, A.J. Westermann, S.A. Gorski, J. Vogel, Single-cell RNA-seq: advances and future challenges, Nucleic Acids Res 42(14) (2014) 8845–60.
9. T. Stuart, R. Satija, Integrative single-cell analysis, Nat Rev Genet 20(5) (2019) 257–272.
10. E. Hedlund, Q. Deng, Single-cell RNA sequencing: Technical advancements and biological applications, Mol Aspects Med 59 (2018) 36–46.
11. X. Zhang, T. Li, F. Liu, Y. Chen, J. Yao, Z. Li, Y. Huang, J. Wang, Comparative Analysis of Droplet-Based Ultra-High-Throughput Single-Cell RNA-Seq Systems, Mol Cell 73(1) (2019) 130-142 e5.
12. G.X. Zheng, J.M. Terry, P. Belgrader, P. Ryvkin, Z.W. Bent, R. Wilson, S.B. Ziraldo, T.D. Wheeler, G.P. McDermott, J. Zhu, M.T. Gregory, J. Shuga, L. Montesclaros, J.G. Underwood, D.A. Masquelier, S.Y. Nishimura, M. Schnall-Levin, P.W. Wyatt, C.M. Hindson, R. Bharadwaj, A. Wong, K.D. Ness, L.W. Beppu, H.J. Deeg, C. McFarland, K.R. Loeb, W.J. Valente, N.G. Ericson, E.A. Stevens, J.P. Radich, T.S.

Mikkelsen, B.J. Hindson, J.H. Bielas, Massively parallel digital transcriptional profiling of single cells, Nat Commun 8 (2017) 14049.

13. H. Su, N. Na, X. Zhang, Y. Zhao, The biological function and significance of CD74 in immune diseases, Inflamm Res 66(3) (2017) 209–216.
14. S.M. Yoon, T. Haritunians, S. Chhina, Z. Liu, S. Yang, C. Landers, D. Li, B.D. Ye, D. Shih, E.A. Vasiliauskas, A. Ippoliti, S. Rabizadeh, S.R. Targan, G.Y. Melmed, D.P.B. McGovern, Colonic Phenotypes Are Associated with Poorer Response to Anti-TNF Therapies in Patients with IBD, Inflamm Bowel Dis 23(8) (2017) 1382–1393.
15. A. Ochi, D. Chen, W. Schulte, L. Leng, N. Moeckel, M. Piecychna, L. Averdunk, C. Stoppe, R. Bucala, G. Moeckel, MIF-2/D-DT enhances proximal tubular cell regeneration through SLPI- and ATF4-dependent mechanisms, Am J Physiol-Renal 313(3) (2017) F767-F780.
16. S. Almaani, A. Meara, B.H. Rovin, Update on Lupus Nephritis, Clin J Am Soc Nephro 12(5) (2017) 825–835.
17. Y. Zhou, H.M. Chen, L. Liu, X.Q. Yu, G.K. Sukhova, M. Yang, L.J. Zhang, V.C. Kyttaris, G.C. Tsokos, I.E. Stillman, T. Ichimura, J.V. Bonventre, P. Libby, G.P. Shi, CD74 Deficiency Mitigates Systemic Lupus Erythematosus-like Autoimmunity and Pathological Findings in Mice, Journal of Immunology 198(7) (2017) 2568–2577.
18. S. Lapter, H. Ben-David, A. Sharabi, H. Zinger, A. Telerman, M. Gordin, L. Leng, R. Bucala, I. Shachar, E. Mozes, A role for the B-cell CD74/macrophage migration inhibitory factor pathway in the immunomodulation of systemic lupus erythematosus by a therapeutic tolerogenic peptide, Immunology 132(1) (2011) 87–95.
19. R. Abe, T. Shimizu, A. Ohkawara, J. Nishihira, Enhancement of macrophage migration inhibitory factor (MIF) expression in injured epidermis and cultured fibroblasts, Biochim Biophys Acta 1500(1) (2000) 1–9.
20. T. Lucas, A. Waisman, T. Krieg, S. Eming, Differential Roles of Macrophages in Diverse Phases of Skin Repair, Wound Repair and Regeneration 18(6) (2010) A88-A88.
21. S. Ensan, A. Li, R. Besla, N. Degousee, J. Cosme, M. Roufaiel, E.A. Shikatani, M. El-Maldizil, J.W. Williams, L. Robins, C. Li, B. Lewis, T.J. Yun, J.S. Lees, P. Wieghofer, R. Khattar, K. Farrokhil, J. Byrne, M. Ouzounian, C.C.J. Zavitz, G.A. Levy, C.M.T. Bauer, P. Libby, M. Husain, F.K. Swirski, C. Cheong, M. Prinz, I. Hilgendorf, G.J. Randolph, S. Epelman, A.O. Gramolini, M.I. Cybulsky, B.B. Rubin, C.S. Robbins, Self-renewing resident arterial macrophages arise from embryonic CX3CR1(+) precursors and circulating monocytes immediately after birth, Nat Immunol 17(2) (2016) 159–168.
22. C.M.L. Beckers, K.R. Simpson, K.J. Griffin, J.M. Brown, L.T. Cheah, K.A. Smith, J. Vacher, P.A. Cordell, M.T. Kearney, P.J. Grant, R.J. Pease, Cre/lox Studies Identify Resident Macrophages as the Major Source of Circulating Coagulation Factor XIII-A, Arterioscl Throm Vas 37(8) (2017) 1494-+.
23. C. Cochain, E. Vafadarnejad, P. Arampatzi, J. Pelisek, H. Winkels, K. Ley, D. Wolf, A.E. Saliba, A. Zernecke, Single-Cell RNA-Seq Reveals the Transcriptional Landscape and Heterogeneity of Aortic Macrophages in Murine Atherosclerosis, Circ Res 122(12) (2018) 1661–1674.

24. Z. Semnani-Azad, S.B. Mejia, P.W. Connelly, R.P. Bazinet, R. Retnakaran, D.J.A. Jenkins, S.B. Harris, A.J. Hanley, The association of soluble CD163, a novel biomarker of macrophage activation, with type 2 diabetes mellitus and its underlying physiological disorders: A systematic review, Obes Rev 22(9) (2021).
25. M. Liguori, E. Digifico, A. Vacchini, R. Avigni, F.S. Colombo, E.M. Borroni, F.M. Farina, S. Milanesi, A. Castagna, L. Mannarino, I. Craparotta, S. Marchini, E. Erba, N. Panini, M. Tamborini, V. Rimoldi, P. Allavena, C. Belgiovine, The soluble glycoprotein NMB (GPNMB) produced by macrophages induces cancer stemness and metastasis via CD44 and IL-33, Cell Mol Immunol 18(3) (2021) 711–722.
26. B. Yu, T. Alboslemy, F. Safadi, M.H. Kim, Glycoprotein Nonmelanoma Clone B Regulates the Crosstalk between Macrophages and Mesenchymal Stem Cells toward Wound Repair, Journal of Investigative Dermatology 138(1) (2018) 219–227.
27. L. Florin, J. Knebel, P. Zigrino, B. Vonderstrass, C. Mauch, M. Schorpp-Kistner, A. Szabowski, P. Angel, Delayed wound healing and epidermal hyperproliferation in mice lacking JunB in the skin, J Invest Dermatol 126(4) (2006) 902–11.
28. M. Honda, B.G.J. Surewaard, M. Watanabe, C.C. Hedrick, W.Y. Lee, K. Brown, K.D. McCoy, P. Kubes, Perivascular localization of macrophages in the intestinal mucosa is regulated by Nr4a1 and the microbiome, Nat Commun 11(1) (2020).
29. S.L. Teitelbaum, F.P. Ross, Genetic regulation of osteoclast development and function, Nat Rev Genet 4(8) (2003) 638–49.
30. M.C. Walsh, N. Kim, Y. Kadono, J. Rho, S.Y. Lee, J. Lorenzo, Y. Choi, Osteoimmunology: interplay between the immune system and bone metabolism, Annu Rev Immunol 24 (2006) 33–63.
31. C.C. Song, X.B. Yang, Y.S. Lei, Z. Zhang, W.L. Smith, J.L. Yan, L.B. Kong, Evaluation of efficacy on RANKL induced osteoclast from RAW264.7 cells, J Cell Physiol 234(7) (2019) 11969–11975.
32. H.X. Zheng, J. Chen, Y.X. Zu, E.Z. Wang, S.S. Qi, Chondroitin Sulfate Prevents STZ Induced Diabetic Osteoporosis through Decreasing Blood Glucose, AntiOxidative Stress, Anti-Inflammation and OPG/RANKL Expression Regulation, Int J Mol Sci 21(15) (2020).
33. K. Asadipooya, E.M. Uy, Advanced Glycation End Products (AGEs), Receptor for AGEs, Diabetes, and Bone: Review of the Literature, J Endocr Soc 3(10) (2019) 1799–1818.
34. F. Loi, L.A. Cordova, J. Pajarinen, T.H. Lin, Z.Y. Yao, S.B. Goodman, Inflammation, fracture and bone repair, Bone 86 (2016) 119–130.
35. M.S. Shaheen, J.I. Silverberg, Atopic dermatitis is associated with osteoporosis and osteopenia in older adults, J Am Acad Dermatol 80(2) (2019) 550–551.
36. C.Y. Wu, Y.Y. Lu, C.C. Lu, Y.F. Su, T.H. Tsai, C.H. Wu, Osteoporosis in adult patients with atopic dermatitis: A nationwide population-based study, Plos One 12(2) (2017).
37. K. Mizutani, K. Isono, Y. Matsushima, K. Okada, A. Umaoka, S. Iida, K. Habe, K. Hagimori, H. Yamazaki, K. Yamanaka, Inflammatory Skin-Derived Cytokines Accelerate Osteoporosis in Mice with Persistent Skin Inflammation, Int J Mol Sci 21(10) (2020).

38. J.B. Barbaroux, M. Beleut, C. Brisken, C.G. Mueller, R.W. Groves, Epidermal receptor activator of NF-kappaB ligand controls Langerhans cells numbers and proliferation, J Immunol 181(2) (2008) 1103–8.
39. V. Duheron, E. Hess, M. Duval, M. Decossas, B. Castaneda, J.E. Klopper, L. Amoasii, J.B. Barbaroux, I.R. Williams, H. Yagita, J. Penninger, Y. Choi, F. Lezot, R. Groves, R. Paus, C.G. Mueller, Receptor activator of NF-kappaB (RANK) stimulates the proliferation of epithelial cells of the epidermo-pilosebaceous unit, Proc Natl Acad Sci U S A 108(13) (2011) 5342–7.

Figures

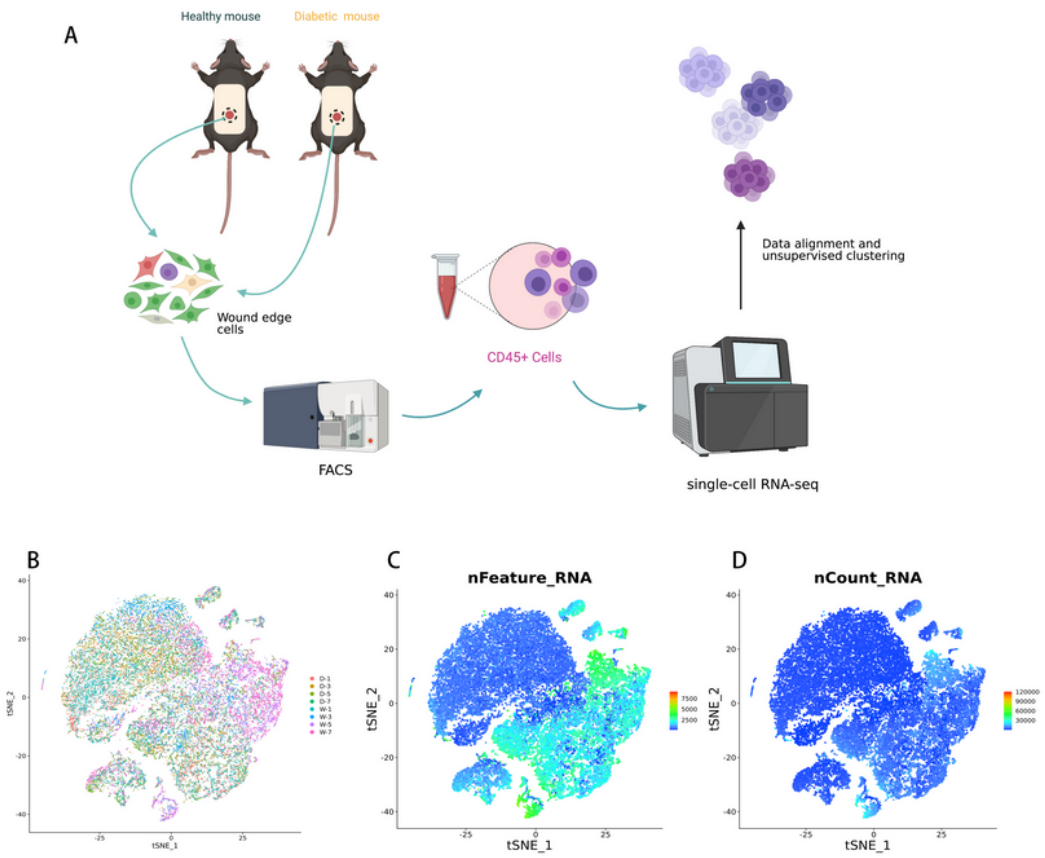

Figure 1

F1 scRNA-seq analysis reveals a dynamic immune landscape in STZ-induced diabetic mouse wounds. (A) Experimental design. Single cell were collected from day1,day3,day5,day7,along wound healing. (B) A t-distributed stochastic neighbour embedding (t-SNE) visualization of all cells displayed with different colours for samples. (C) t-SNE visualization of the gene expression of each cell. (D) t-SNE visualization of the UMI expression of each cell.

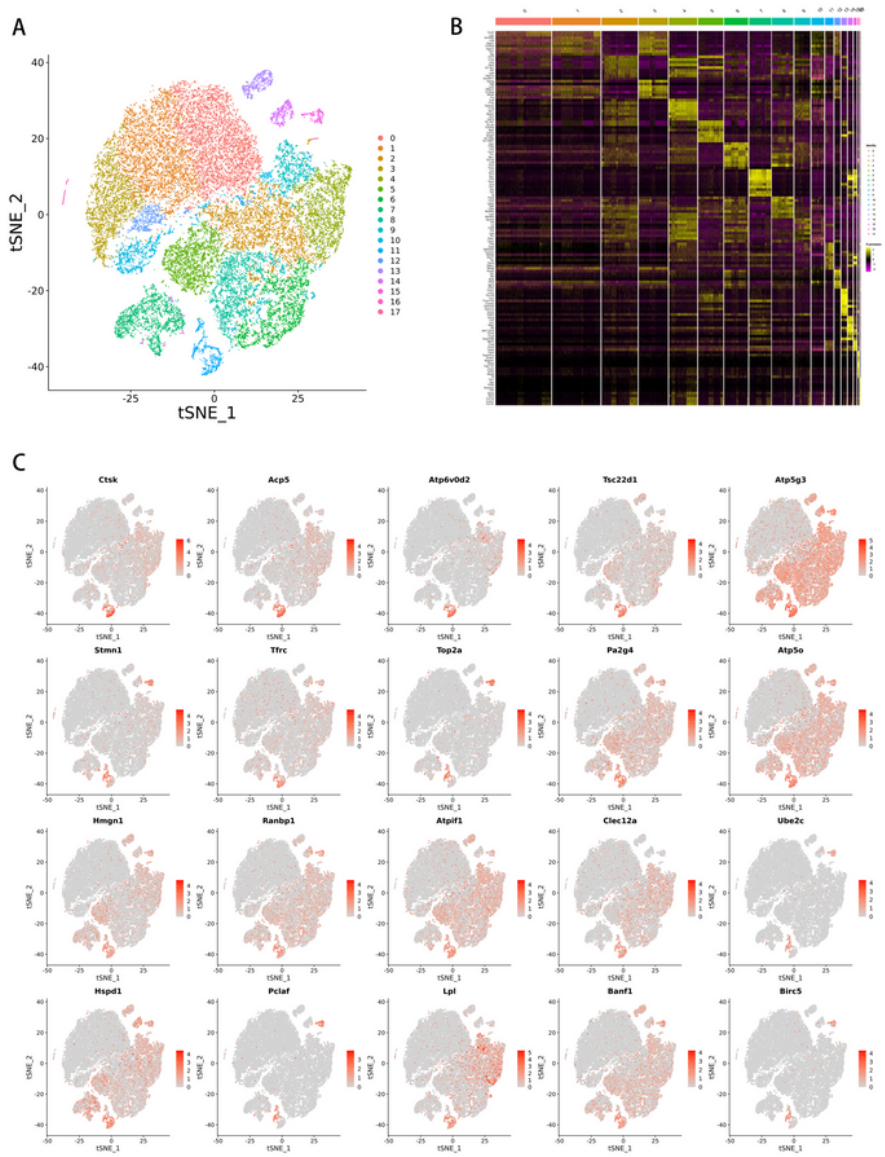

Figure 2

scRNA-seq based identification of STZ-induced diabetic mouse wounds immune cell populations. (A) t-SNE visualization of 9240 single cells, colour-coded by assigned cell type (B) Heat map of all clusters top 20 upregulated marker gene . Shades of colour indicate high or low gene expression, with yellow being high expression and dark red being low expression. (C) Distribution of the top 20 genes in cluster 11 in all cells. Red color indicate high gene expression.

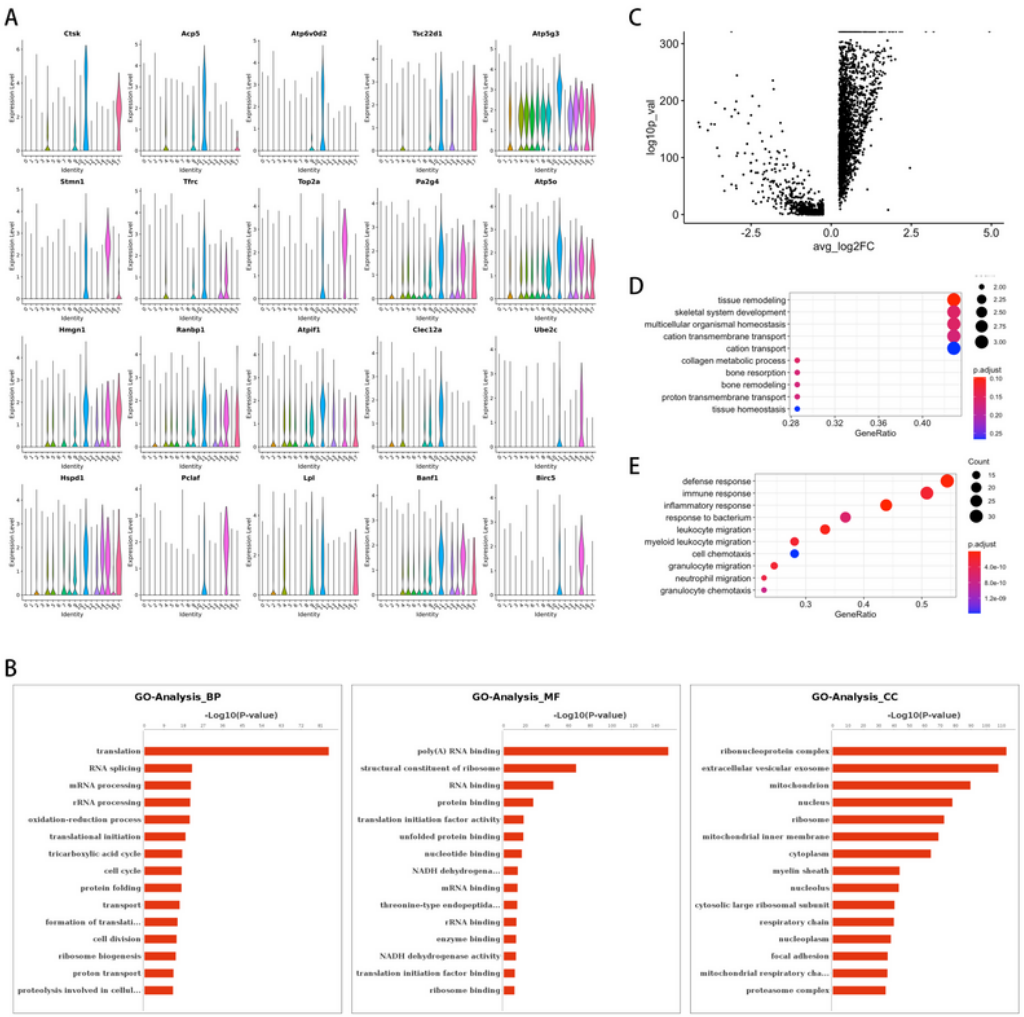

Figure 3

Gene expression characteristics and biological function analysis of cluster 11 and the gene expression differences compared with other macrophages. (A) Violin plot view cluster11 top 20 marker gene demonstrating overall gene expression. The number of identity is the same of clusters. (B) GO histogram analysis results of cluster11 marker gene: Biological Process(BP),Molecular (MF), Cellular Component(CC). Coordinate axis Y: Go-Term entry name,Coordinate axis X: -log10 (P-Value). Red for

significant entries, blue for non-significant entries. (C) Volcano plot view for the gene expression difference between cluster11 and other macrophages(cluster2,4,9).Coordinate axis Y: -log10(P-Value), axis X:avg_log2FC.X<-1 use pink color as down expression, X>1 use blue color as up expression. (D) GO analysis up regulated and down regulated gene(E) of cluster11: Biological Process, Coordinate axis Y: Go-Term entry name,Coordinate axis X: Gene Ratio. Colors of the bubble represents P.adjust<0.05 for significant entries. The size of the bubble indicates the number of genes enriched in this item.

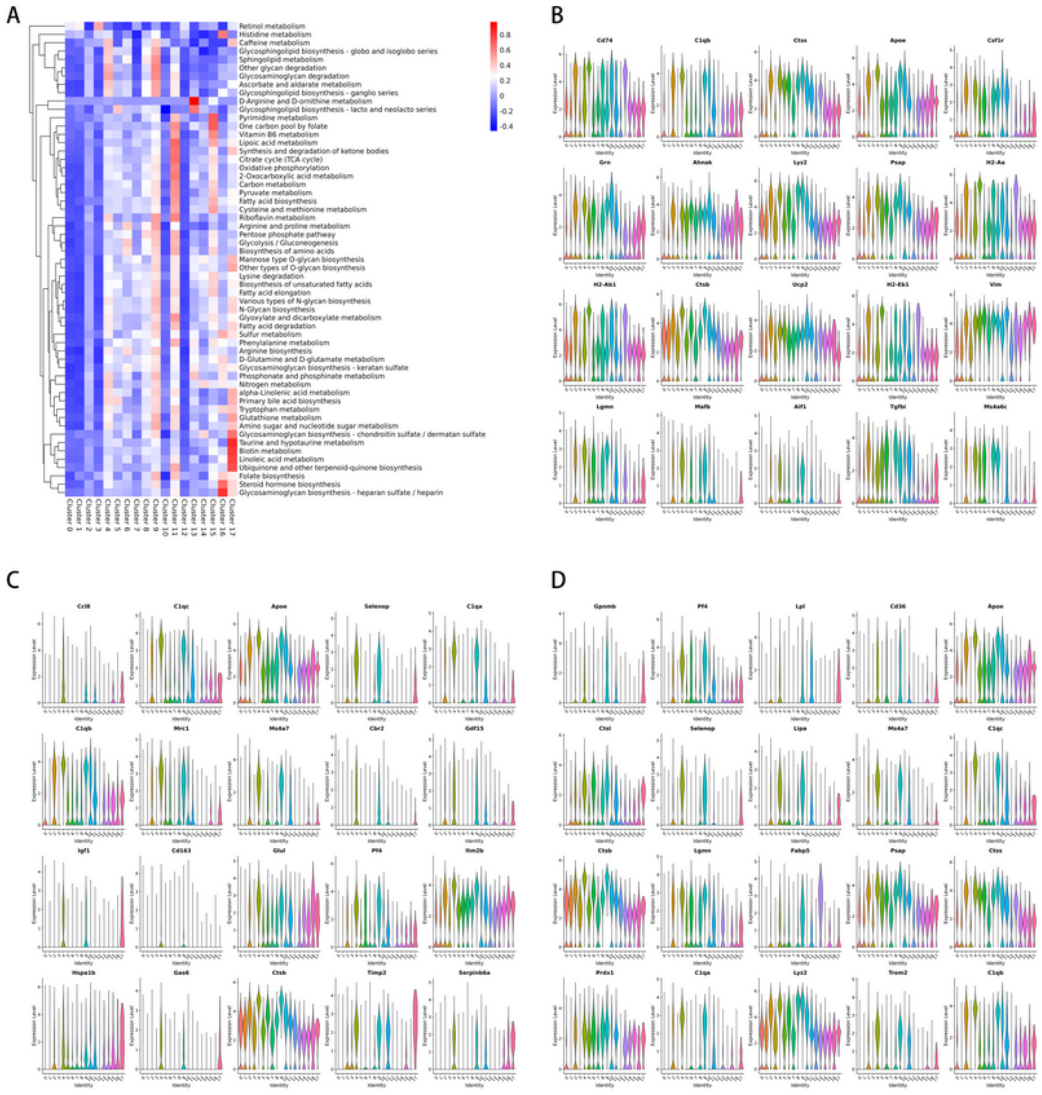

Figure 4

Macrophage gene metabolism pattern analysis (A) Heatmap of Qusage Analysis, shows the significance of enrichment between cluster in metabolism gene set.Axis Y: Gene set information,aixs X:clusters. The colour represents the significance of each cluster in each gene set, the closer the colour to red, the more significant it is; the closer the colour to blue, the less significant it is. (B) Violin plot view cluster2 top 20 marker gene demonstrating overall gene expression. (C) Violin plot view cluster4 top 20 marker gene demonstrating overall gene expression. (D) Violin plot view cluster9 top 20 marker gene demonstrating overall gene expression.

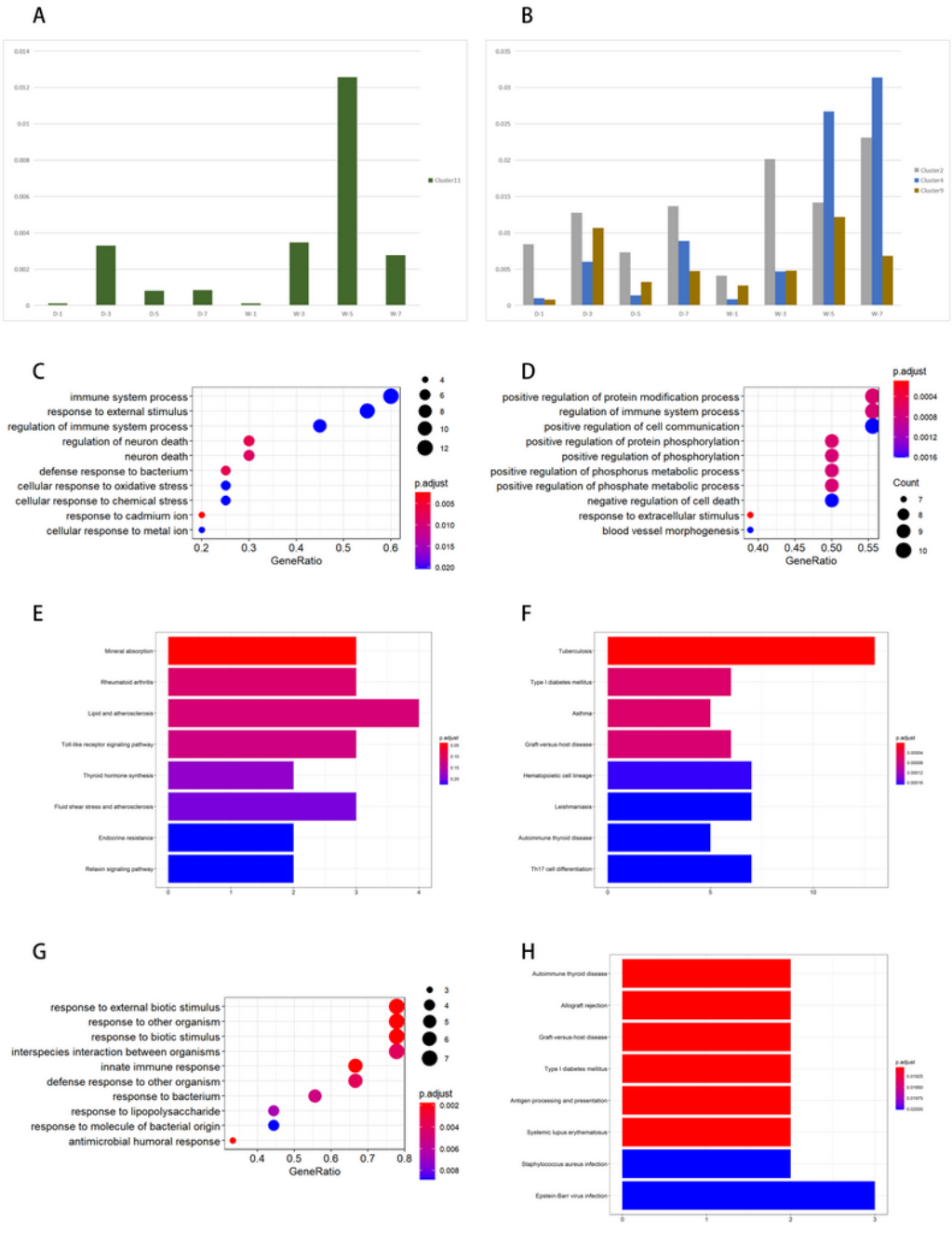

Figure 5

Differences in the proportion of macrophages over time and the differences in gene expression between the diabetic wound group and the control group (A) The proportion of cluster 11 cells in the control group on day 5 and day 7 was much higher than diabetic group. Coordinate axis Y: Proportion of specific cluster of cells in all single cells, Coordinate axis X: cell clusters, group and sampling time. Ex: D-1(Diabetic group -day 1), W-1(Wild type control group-day 1). (B) The proportion of cluster 2, cluster 4, and cluster 9 cells in the control group and diabetic group. (C) GO enrichment analysis of the differential genes and found that the differences in the biological functions between the two groups with respect to cluster 11 on day 3 (D) GO enrichment analysis of the downregulated genes in cluster 11 on day 5 in the diabetes group and the biological functions of the differences. (E) KEGG terms of control and diabetes two groups of cluster 11 cells on day 3 differentially expressed genes. (F) KEGG terms of the cluster 11 cells on day 7 upregulated genes in the diabetes group. (G) GO enrichment analysis of the upregulated genes in cluster 4 on day 5 in the diabetic group and the biological functions of the differences. (H) KEGG enriched differential gene pathways on day 5 of cluster 4.

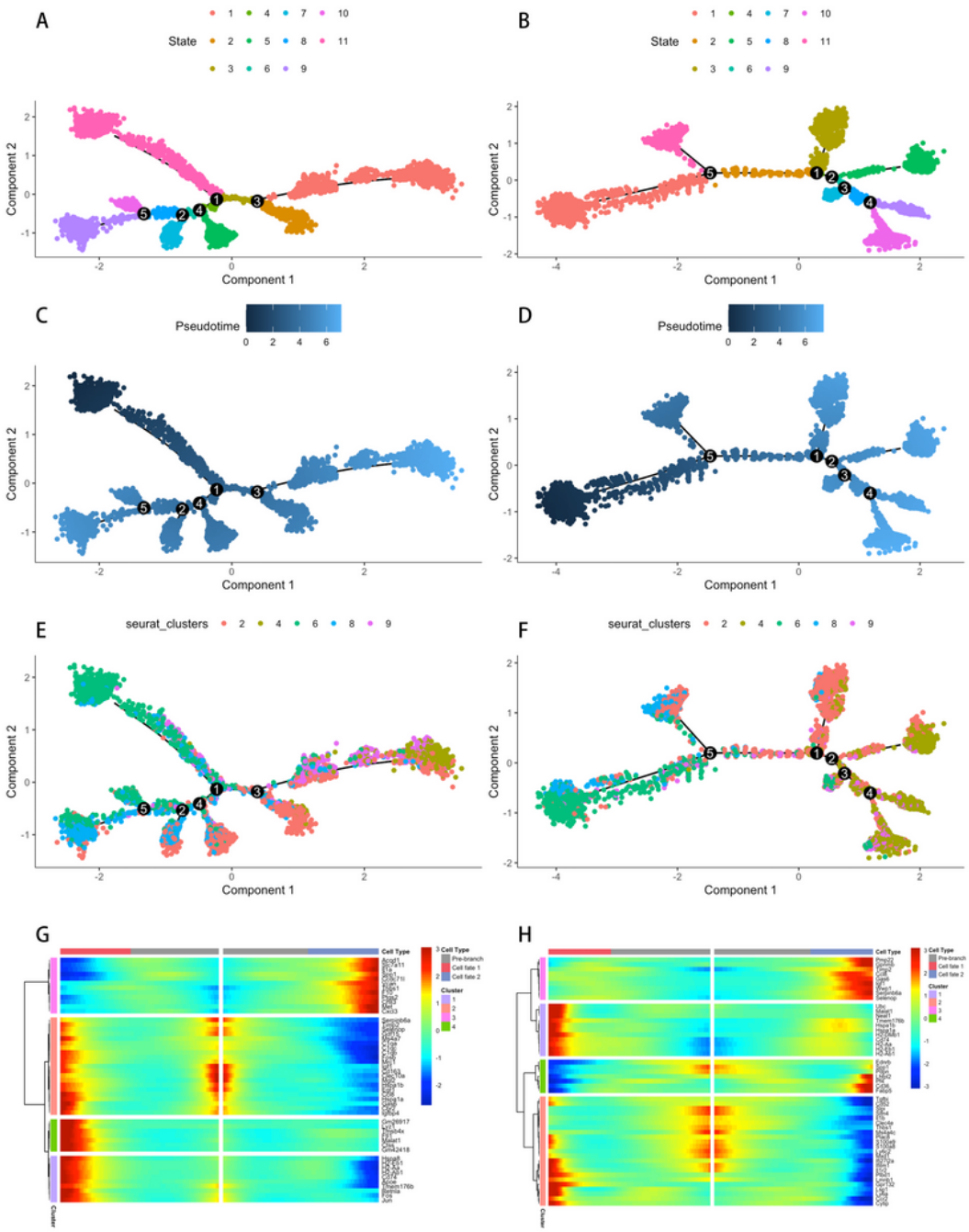

Figure 6

Pseudotime analysis of macrophage populations and analysis of the differential gene expression patterns in the developmental branches. (A, B) Reconstruction of the monocyte/macrophage trajectory as 11 state. Control group(A), Diabetes group(B). (C, D) Reconstruction of the monocyte/macrophage trajectory in a pseudotime manner.

Supplementary Files

This is a list of supplementary files associated with this preprint. Click to download.

- supplementary1.png
- supplementary2.png
- supplementary3.png